

Contrast settling in cerebral aneurysm angiography

Zhi-Jie Wang^{1,2}, Kenneth R Hoffmann^{1,3}, Zhou Wang¹,
Stephen Rudin^{1,2,3,4}, Lee R Guterman^{1,3} and Hui Meng^{1,2,3}

¹ Toshiba Stroke Research Center, University at Buffalo, State University of New York,
3435 Main Street, 445 BRB, Buffalo, NY 14214, USA

² Department of Mechanical & Aerospace Engineering, University at Buffalo,
State University of New York, 324 Jarvis Hall, Buffalo, NY 14260, USA

³ Department of Neurosurgery, University at Buffalo, State University of New York,

3 Gates Circle, Buffalo, NY 14209, USA

⁴ Departments of Physiology and Biophysics, Radiology, Physics, University at Buffalo,
State University of New York, 3435 Main Street, 445 BRB, Buffalo, NY 14214, USA

E-mail: huiMeng@eng.buffalo.edu

Received 6 January 2005, in final form 7 April 2005

Published 22 June 2005

Online at stacks.iop.org/PMB/50/3171

Abstract

During angiography, blood flow is visualized with a radiopaque contrast agent, which is denser than blood. In complex vasculature, such as cerebral saccular aneurysms, the density difference may produce an appreciable gravity effect, where the contrast material separates from blood and settles along the gravity direction. Although contrast settling has been occasionally reported before, the fluid mechanics behind it have not been explored. Furthermore, the severity of contrast settling in cerebral aneurysms varies significantly from case to case. Therefore, a better understanding of the physical principles behind this phenomenon is needed to evaluate contrast settling in clinical angiography. In this study, flow in two identical groups of sidewall aneurysm models with varying parent-vessel curvature was examined by angiography. Intravascular stents were deployed into one group of the models. To detect contrast settling, we used lateral view angiography. Time-intensity curves were analysed from the angiographic data, and a computational fluid dynamic analysis was conducted. Results showed that contrast settling was strongly related to the local flow dynamics. We used the Froude number, a ratio of flow inertia to gravity force, to characterize the significance of gravity force. An aneurysm with a larger vessel curvature experienced higher flow, which resulted in a larger Froude number and, thus, less gravitational settling. Addition of a stent reduced the aneurysmal flow, thereby increasing the contrast settling. We found that contrast settling resulted in an elevated washout tail in the time-intensity curve. However, this signature is not unique to contrast settling. To determine whether contrast settling is present, a lateral view should be obtained in addition to the anteroposterior (AP) view routinely used clinically so as to rule out contrast settling and

hence to enable a valid time-intensity curve analysis of blood flow in the aneurysm.

(Some figures in this article are in colour only in the electronic version)

1. Introduction

In x-ray angiography, contrast agents are commonly used to opacify the vessel lumen and quantify blood flow (Shroy *et al* 2000, Smedby 1992, Shpilfoygel *et al* 2000). When using a contrast agent as an intravascular flow tracer, one implicitly assumes that this contrast flow represents the blood flow. This assumption may not always be valid, because contrast agents used in angiography are denser than blood. The density difference can produce an appreciable gravity effect, leading to the so-called contrast settling identified in radiographic imaging (Schoepf *et al* 2000, Tarver and Plant 1995, Clough *et al* 2003), where the contrast material separates from blood and settles along the gravity direction.

At our institution, contrast settling was observed during biplane cerebral angiography of a giant aneurysm (figure 1) in a 56-year-old woman who presented with double vision. During a biplane angiographic acquisition, a bolus of contrast (density = 1.405 g cm^{-3} , viscosity = 9.0 cPs, Optiray[®] 350, Mallinckrodt Inc., St. Louis, MO) was injected. Figure 1 shows the anteroposterior (AP) views (figure 1(a)) and the lateral views (figure 1(b)) of a large left posterior inferior cerebellar artery aneurysm in which the sac is oriented in a downward position. In each view, we show snapshots acquired during the early filling stage ($t = 1.8 \text{ s}$) and at the end of recording ($t = 7.9 \text{ s}$). The routine AP view shows a significant amount of contrast 'stasis' within the aneurysm. Based on previous work, this would indicate very slow refreshment of the blood in the sac that promotes thrombosis (Wakhloo *et al* 1994, Geremia *et al* 1994). However, the lateral view in the figure clearly shows that the apparent 'stasis' was actually caused by gravity leading to contrast settling at the bottom of the aneurysm sac.

In non-pathological vessels, the gravity effect is usually not a source of concern. However, if the vessel geometry is abnormal, like in a saccular intracranial aneurysm, the gravity effect could produce significant contrast settling. Besides the clinical observation above, we have seen contrast settling in *in vitro* experiments (Wang *et al* 2004). These studies indicated that the severity of contrast settling varied from case to case and tended to be minimized in sidewall aneurysms with strongly curved parent vessels. However, it is still unclear what haemodynamic conditions promote contrast settling. Hence, investigation of the fluid mechanism that dominates such phenomena is needed.

Our previous studies have shown an increased aneurysmal flow with increased parent-vessel curvature (Hoi *et al* 2004), and a decreased aneurysmal flow after stent placement (Wang *et al* 2004). In the current study, we used the same type of aneurysm models, i.e., saccular aneurysms on curved vessels, to examine how the severity of contrast settling is related to the local flow environments, and how it is influenced by vessel geometry and endovascular interventions.

2. Methods

Two identical groups of elastomer sidewall aneurysm models were used (Ionita *et al* 2004) (Sylgard 184, Dow Corning Corporation, Midland, MI). In each group, the parent-vessel curvature was varied, while other parameters remained constant. Details of the model design

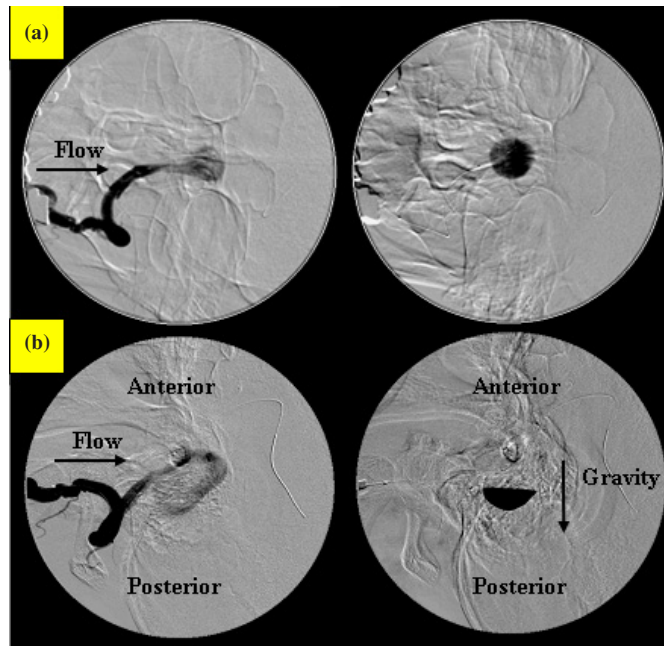


Figure 1. Sequential angiographic imaging of a large left posterior inferior cerebellar artery aneurysm. (a) Anteroposterior (AP) view; (b) Lateral view. The left column shows angiograms at the contrast filling period ($t = 1.8$ s), and the right column shows angiograms at the end of recording ($t = 7.9$ s). The lateral view angiograms reveal significant contrast settling at the end of recording, whereas the AP view shows residue of contrast, which could be interpreted as flow 'stasis'.

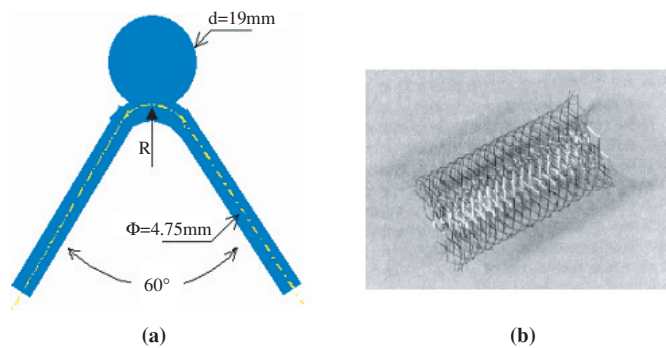


Figure 2. (a) Design of the sidewall aneurysm model. Φ : parent-vessel diameter, R : inverse of parent-vessel curvature, d : aneurysm diameter. (b) Wallstent[®] (Boston Scientific, Natick MA).

are shown in figure 2(a). Parent-vessel curvature was defined as $C = 1/R$, where R is the radius of the curvature of the vessel centreline near the aneurysm. Four different curvatures were created, 0 mm^{-1} (straight), 0.04 mm^{-1} , 0.08 mm^{-1} and 0.1 mm^{-1} . Commercial self-expanding stents were deployed (5×40 mm Wallstent[®], Boston Scientific, Natick, MA, figure 2(b)) across the aneurysm neck in each of four models of one group. In the other group, four non-stented models served as a control.

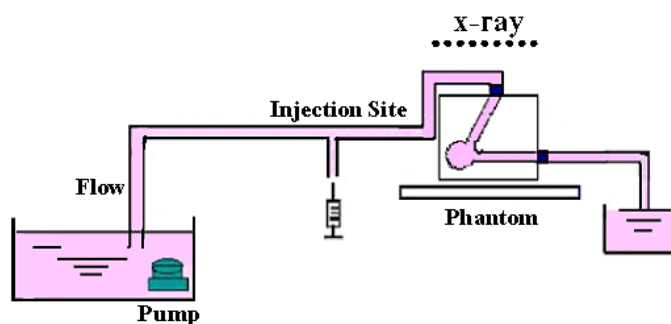


Figure 3. Schematic of the flow loop.

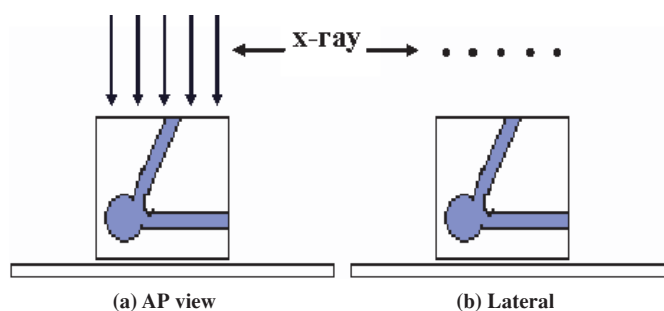


Figure 4. Two modes of angiogram acquisition. (a) AP view. The x-ray beam is indicated by the arrows. (b) Lateral view. The x-ray beam coming out of the paper plane is marked as dots.

The working fluid was a 60/40 mixture of glycerin and water. The fluid had a density of 1.157 g cm^{-3} and a viscosity of 15.2 cP ($1 \text{ cP} = 0.001 \text{ Pa s}$). By comparison, whole blood has a density of 1.06 g cm^{-3} and a viscosity of 3.5 cP . The contrast media used was OXILANTM 300 (Cook Imaging Co., Bloomington, Indiana) with a density of 1.303 g cm^{-3} and a viscosity of 9.4 cP . A flow loop was set up as shown in figure 3. Pulsatile flow was generated by a pump equipped with MasterFlex[®] L/S[®] Easy-Load[®] heads (Cole-Parmer Instrument Co., Vernon Hills, Illinois). The average flow rate was 260 ml min^{-1} , and the pulse frequency was 1.25 Hz .

During the experiment, the aneurysms were oriented posteriorly relative to the vessel, as shown in figure 4. Instead of using the routine AP view (figure 4(a)), we acquired lateral views (figure 4(b)), which allowed not only the calculation of time-intensity curves but also the visualization of contrast settling. For flow visualization, 4 ml contrast material was injected manually at an injection rate of approximately 4 ml s^{-1} . The variations in hand injections were examined by recording the time-intensity curve of the contrast in the upstream parent-vessel region of each run. These waveforms were found to overlap with each other, suggesting that variations in hand injections could be neglected.

The x-ray angiography-imaging system was a ceiling-mounted C-arm, model CAS-8000V (Toshiba Medical Systems Corp., Tokyo, Japan). The acquisition rate was $15 \text{ frames per second}$ (fps) for the wash-in period (first 3 s), and was reduced to 3 fps for the washout period (the subsequent 10 s). The x-ray parameters were set to 70 kVp , $80\text{--}100 \text{ mA}$, with Automatic Exposure Control.

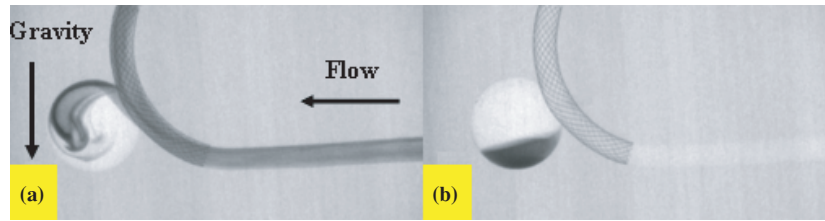


Figure 5. Images from an angiographic sequence in a stented model with a vessel curvature of 0.04 mm^{-1} . (a) $t = 1.53 \text{ s}$. (b) $t = 13 \text{ s}$.

To characterize the aneurysmal flow from the angiograms, we calculated the average grey level of the region of interest (ROI) as a function of time, $c'(t)$. This ROI consisted of the entire aneurysm sac. Each curve was then normalized using

$$c(t) = \frac{c'(t) - c_{\min}}{c_{\max} - c_{\min}}, \quad (1)$$

where $c_{\min} = \text{Min}(c'(t))$, $c_{\max} = \text{Max}(c'(t))$, and $c(t)$ is the normalized intensity at time. The $c(t)$ plot is referred to as the time-intensity curve. In this study, we assumed that the pixel value (intensity) was linearly related to the concentration of contrast and evaluated the time-intensity curves. Typically, the contrast value in the ROI rises rapidly as contrast flows into the aneurysm, followed by a slower decrease during the washout of the contrast. We estimated the relative amount of contrast material remaining in the aneurysm at the end of the recording by averaging the grey values in the ROI over the last three angiograms.

To further identify how the flow dynamics affects contrast settling, the flow was quantified in terms of the Froude number, which represents the relative importance of the local flow inertia against the gravity force. Mathematically, the Froude number (Hung *et al* 1980) is defined as

$$\text{Fr} = \frac{V}{\sqrt{gL(\rho_c - \rho_b)/\rho_b}}, \quad (2)$$

where V is the blood flow velocity, L is the length scale, ρ_c and ρ_b are the densities of contrast and blood respectively (in our study, $\rho_c = 1.303 \text{ g cm}^{-3}$, $\rho_b = 1.157 \text{ g cm}^{-3}$) and g is the acceleration of gravity ($g = 9.8 \text{ m s}^{-2}$). In this study, V was taken as the average flow velocity inside the aneurysm, and L was the diameter of the aneurysm sac.

To obtain the aneurysm flow velocity V in stented models, we performed computational fluid dynamic (CFD) analysis using a commercial finite volume code, STARCD[®] (Adapco, Melville, NY). The same model geometry, fluid properties and flow rate as used in the angiographic flow experiment were applied to the computational model. A stent with the same porosity as a Wallstent was implanted across the aneurysm neck in the computational model. A steady-state parabolic velocity profile was applied at the inlet of the model. Each model consisted of 1.8 million tetrahedral meshes.

The CFD simulations provided the three-dimensional flow fields of the stented models. The average flow velocity obtained from the simulation was then used to compute the Froude number in each model.

3. Results

3.1. Lateral view showing contrast settling

An example of a lateral angiographic acquisition showing contrast pooling in a stented aneurysm model (vessel curvature = 0.04 mm^{-1}) is presented in figure 5. The vortex-like flow

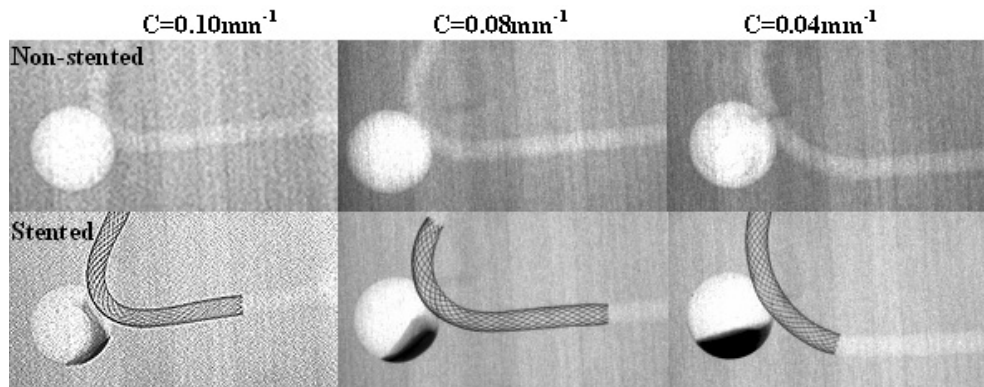


Figure 6. The effect of vessel curvature on contrast settling is directly visualized on the final images of angiographic sequences. Top: non-stented models; Bottom: stented models. The amount of contrast residue increases with decreasing vessel curvature. Variations in stent length and position among different models do not produce appreciable changes in aneurysmal flow.

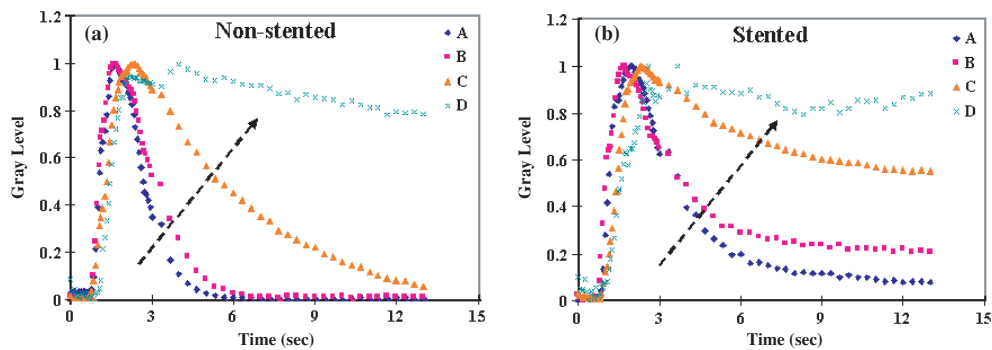


Figure 7. Time-intensity curves in non-stented (a) and stented (b) models. Arrows show the direction of decrease in vessel curvature. Curvatures for these models are: A, 0.10 mm^{-1} ; B, 0.08 mm^{-1} ; C, 0.04 mm^{-1} and D, 0 mm^{-1} .

was apparent in the wash-in image (figure 5(a)). At the end of the acquisition (figure 5(b)), a portion of contrast had settled to the bottom.

Figure 6 shows the final angiograms for non-stented and stented curved-vessel aneurysm models. There was no contrast settled in the non-stented models; however, contrast settling was observed in all the stented models. Moreover, the amount of contrast retained increased as the parent-vessel curvature decreased.

3.2. Time-intensity curve analysis for contrast settling

Besides direct visualization, the time-intensity data also indicated contrast settling. Figure 7 shows the time-intensity curves $c(t)$ for the non-stented and stented models. All the curves in the stented models and non-stented straight vessel model remained above zero at the end of the sequence, indicating a contrast residue in the aneurysm. On the other hand, non-stented curved geometries had no contrast residue. Moreover, a smaller vessel curvature was associated with a slower washout rate, whereby the tail of the time-intensity curve ended at a higher grey level. Figure 8 shows contrast residue determined from the time-intensity curves (figure 7) as a

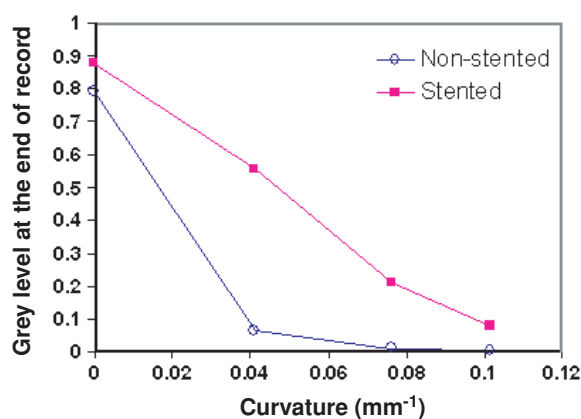


Figure 8. Comparison of contrast residue grey levels measured from normalized time-intensity curves. As vessel curvature increases, less contrast remains at the end of the recording. Stenting produces an increase of contrast settling.

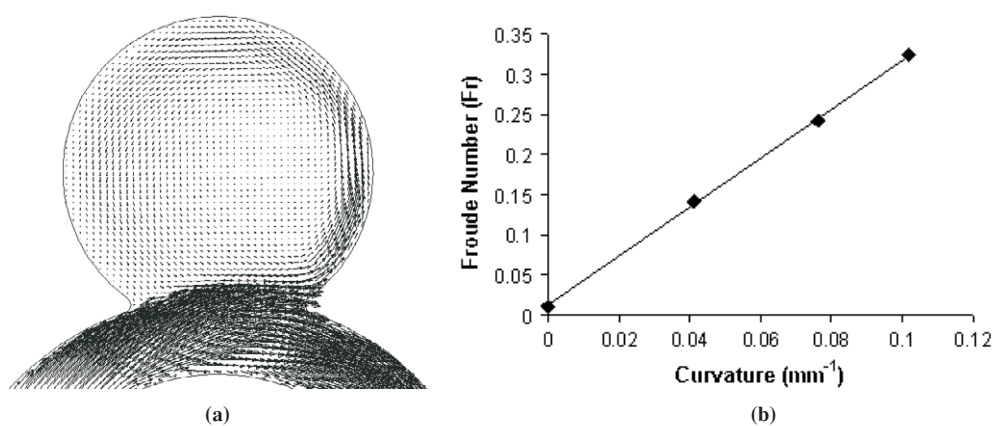


Figure 9. CFD simulation and Froude number (Fr) calculation. (a) 2D velocity field at the centre plane of the aneurysm model with the curvature of 0.04 mm^{-1} . Inlet velocity for the CFD simulation was taken from experiment. From the simulation results, the average velocity in the aneurysm sac was calculated for each Froude number. However, only the detailed flow pattern for one curvature is shown here. (b) The Froude number of four different stented aneurysm models derived from average velocities calculated from CFD simulation.

function of vessel curvature. As the curvature decreased, contrast residue increased. Stenting resulted in an increase in contrast residue.

3.3. Froude number calculations in stented aneurysm models

The stented aneurysm models used in the experiment were analysed by CFD simulations. It was found that, for smaller curvatures, the aneurysm flow was weaker and the residence time of fluid inside the aneurysm was longer. This finding is consistent with the results for non-stented aneurysm models in a previous study (Hoi *et al* 2004). Figure 9(a) gives an example of the centre-plane 2D velocity field in a stented aneurysm model with the curvature of 0.04 mm^{-1} from our 3D CFD simulations. The effect of vessel curvature on Froude number is

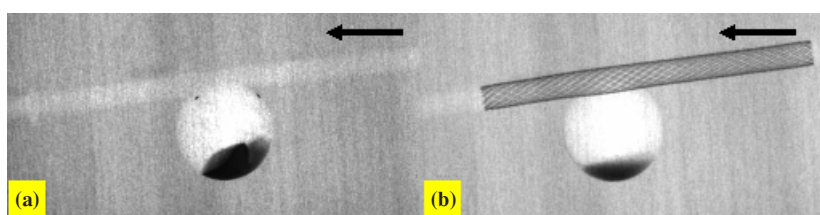


Figure 10. Contrast settling in straight vessel aneurysm models. (a) Non-stented. (b) Stented. The absolute amount of contrast residue is less after stent placement.

shown in figure 9(b). The Froude number increased linearly as the vessel curvature increased, indicating a decreasing effect of gravity. This is consistent with results shown in figure 6.

3.4. Sidewall aneurysm on a straight vessel: a special case

Figure 10 shows contrast settling in non-stented and stented sidewall aneurysms on straight vessels. It demonstrates unusual characteristics as compared to the curved models (figure 6). Substantial contrast settling was seen with and without stent placement. In both cases, contrast entered the cavity and stayed there until the end of acquisition—no portion of it was washed out. Furthermore, figure 8 shows that for the zero curvature model (straight vessel) stenting did not increase the amount of contrast residue as much as expected from the trend of data acquired from the other models. Moreover, despite the increased relative value on the normalized time-intensity curve, $c(t)$, we could see from figure 10 that the *absolute* amount of contrast residue in the straight vessel model actually decreased following the stent placement.

4. Discussion

4.1. The detection of contrast settling

Clinically, contrast flow has been used extensively to document anatomical structures and analyse blood flows qualitatively. Because of different densities and other physical properties, contrast media should be considered more as a ‘marker’ than as a ‘replica’ of the blood flow. In particular, caution should be given to differentiating contrast settling by gravitation from the trapping of contrast media in a recirculation flow by a vortex. To correctly interpret the blood flow of cerebral aneurysms from angiography, it is important to know whether gravitational contrast settling is present.

The time-intensity curve technique has been established to indicate the flow dynamics in a region of interest, e.g., cerebral aneurysms (Tenjin *et al* 1998). Moreover, it has also been explored to evaluate the effectiveness of endovascular intervention in cerebral aneurysms (Sadasivan *et al* 2002). In our study, we obtained the time-intensity curves for each model. We found that contrast settling resulted in an elevated tail on time-intensity curves. However, this ‘signature’ is not unique. In previous studies, an elevated tail has been seen and attributed to recirculation in a perfusion bed (Lawson *et al* 1999, Lee *et al* 1997) or vortex flow (Sadasivan *et al* 2002) in an aneurysm. The contrast agent would have been washed out and the time-intensity curve returned to zero eventually, had the recording time been sufficiently long. Thus, within a limited recording window of a time-intensity curve, one would not know whether the elevated tail were the result of contrast settling or simply a segment of a long washout process.

Our study suggests that the lateral view projection can accurately determine the presence of contrast settling. From an AP view, contrast settling cannot be ascertained, because the x-ray projection is parallel to the direction of gravity. On the other hand, a cross-table lateral view clearly shows the level interface between settled contrast material and blood in the aneurysm, as demonstrated by this study.

4.2. Contrast settling and Froude number

Contrast settling is strongly dependent on blood flow dynamics. When the flow velocity is high, contrast tends to be carried downstream by flow inertia rather than settling in a cavity. To quantify the relationship between contrast settling and the local haemodynamics, we employ the Froude number, which compares the relative magnitude of flow inertia force to gravitational force in multi-species flows (e.g., contrast–blood mixture).

At high Froude numbers ($Fr > 0.5$), the flow inertia is predominate and contrast settling is negligible. At low Froude numbers ($Fr < 0.5$), the gravity force is predominate and contrast settling is pronounced (Hung *et al* 1980). For given contrast and blood densities, a low Froude number implies a slow flow (equation (2)). It follows that the presence of strong contrast settling indicates flow stagnancy.

4.3. Contrast settling in aneurysm flow

In cerebral aneurysms, anatomical factors, such as parent-vessel curvature, have been found to greatly affect the local haemodynamics (Niimi *et al* 1984, Liou and Liao 1997, Hoi *et al* 2004). A higher curvature produces stronger flow impingement at the distal neck and a higher velocity in the aneurysm. This is consistent with the computational results of stented aneurysms in the present study. Aneurysms with larger vessel curvatures have larger Froude numbers (figure 9), thereby experiencing less contrast settling (figure 6).

The present study shows that intraluminal stenting of an aneurysm has the effect of decreasing the contrast washout rates (figure 8) and increasing contrast settling (figures 7 and 9). This can be explained on the basis of the Froude number as well. Previous studies indicated that stenting reduces intra-aneurysmal flow (Lieber *et al* 1997, 2002, Ringer *et al* 2001, Wakhloo *et al* 1994, 1998). An increased gravity effect can be considered a result of lower flow dynamics, as represented by the decreased Froude number.

4.4. Straight vessel aneurysm model

We have shown that, with respect to contrast settling, the straight vessel aneurysm model behaves rather differently from the curved vessel models. While only the addition of stents produced contrast settling in our curved vessel aneurysm models, the straight vessel model always experienced contrast settling, as long as the aneurysm orientation is such that the sac is not directly above the vessel. Our results show that the gravity effect is intrinsically stronger in the straight vessel case. This is due to the different mechanisms that drive the flow into these two types of aneurysms. For a sidewall aneurysm on a curved vessel, the centrifugal force associated with the vessel curvature results in an *inertia-driven* flow into the aneurysm. The higher the curvature, the larger the flow inertia and, hence, less contrast settling (figure 6). For an aneurysm on a straight vessel, there is no inertia flow into the aneurysm; the aneurysmal flow is caused by the viscous shear force at the interface of the aneurysm and parent vessel (Hoi *et al* 2004). This type of *shear-driven* flow is much weaker than the *inertia-driven* flow; therefore, a straight vessel aneurysm model is associated with a rather small Froude number and, hence, a strong gravitational effect.

Another interesting fact we observed in this case was that the increase of contrast settling after stenting was minimal compared with curved vessel models. However, this does not necessarily mean that the reduction of flow was least in the straight vessel models. In fact, we observed that the stent provided the greatest impedance and disturbance to the flow entering aneurysm in this case, consequently providing a conduit for the flow in the straight parent vessel. More contrast material was transported downstream in the vessel rather than into aneurysm cavity. Hence, the total amount of contrast material into the aneurysm was actually less for the stented case.

5. Conclusion

The gravity effect in angiography due to density difference between contrast and blood is mediated by the vascular flow environment, which depends on vascular geometry and interventional device. The contrast settling is related to the local haemodynamics via the Froude number, a ratio of flow inertia and gravity force. The severity of the contrast settling in sidewall cerebral aneurysms increases with decreasing vessel curvature and is strongest for those on straight vessels. Furthermore, the placement of an intravascular stent leads to a considerable increase in contrast settling by reducing the flow inertia into the aneurysm.

Contrast settling is a serious concern in angiogram-based flow analysis of cerebral aneurysms. In the clinical setting, contrast settling may be concealed by a routine anteroposterior view that parallels the gravity direction. Although quantitative analysis of anteroposterior view angiography, such as time-intensity curves, may reveal an elevated washout tail, this is not a unique signature of contrast settling. Therefore, we suggest that biplane angiography, including a lateral view, be used whenever feasible to rule out contrast settling and, hence, to enable valid time-intensity curve analyses of aneurysmal blood flow.

Acknowledgments

We thank Minsuok Kim for providing CFD simulations in the stented aneurysm models. We thank Paul H Dressel for help with preparation of the illustrations and Debi Zimmer and Joanne Smith for editorial assistance. This work is supported by National Science Foundation grant BES-0302389.

References

- Clough A V, Haworth S T, Roerig D L, Hoffman E A and Dawson C A 2003 Influence of gravity on radiographic contrast material-based measurements of regional blood flow distribution *Acad. Radiol.* **10** 128–38
- Geremia G, Haklin M and Brennecke L 1994 Embolization of experimentally created aneurysms with intravascular stent devices *AJNR. Am. J. Neuroradiol.* **15** 1223–31
- Hoi Y, Meng H, Woodward S, Bendok B R, Hanel R A, Guterman L R and Hopkins L N 2004 Effects of arterial geometry on aneurysm growth: three-dimensional computational fluid dynamics study *J. Neurosurg.* **101** 676–81
- Hung T C, Hung T K and Bugliarello G 1980 Blood flow in capillary tubes: curvature and gravity effects *Biorheology* **17** 331–42
- Ionita C N, Hoi Y, Meng H and Rudin S 2004 Particle image velocimetry (PIV) evaluation of flow modification in aneurysm phantoms using asymmetric stents *Proc. SPIE* **5369** 295–306
- Lawson R S 1999 Application of mathematical methods in dynamic nuclear medicine studies *Phys. Med. Biol.* **44** R57–98
- Lee E T, Rehkopf P G, Warnicki J W, Friberg T, Finegold D N and Cape E G 1997 A new method for assessment of changes in retinal blood flow *Med. Eng. Phys.* **19** 125–30
- Lieber B B and Gounis M J 2002 The physics of endoluminal stenting in the treatment of cerebrovascular aneurysms *Neurol. Res.* **24** (Suppl 1) S33–42

- Lieber B B, Stancampiano A P and Wakhloo A K 1997 Alteration of hemodynamics in aneurysm models by stenting: influence of stent porosity *Ann. Biomed. Eng.* **25** 460–9
- Liou T M and Liao C C 1997 Flowfields in lateral aneurysm models arising from parent vessels with different curvatures using PTV *Exp. Fluids* **23** 288–98
- Niimi H, Kawano Y and Sugiyama I 1984 Structure of blood flow through a curved vessel with an aneurysm *Biorheology* **21** 603–15
- Ringer A J, Lopes D K, Boulos A S, Guterman L R and Hopkins L N 2001 Current techniques for endovascular treatment of intracranial aneurysms *Semin. Cerebrovasc. Dis. Stroke* **1** 39–51
- Sadasivan C, Lieber B B, Gounis M J, Lopes D K and Hopkins L N 2002 Angiographic quantification of contrast medium washout from cerebral aneurysms after stent placement *AJNR. Am. J. Neuroradiol.* **23** 1214–21
- Schoepf U J *et al* 2000 Pulmonary embolism: comprehensive diagnosis by using electron-beam CT for detection of emboli and assessment of pulmonary blood flow *Radiology* **217** 693–700
- Shpilfoygel S D, Close R A, Valentino D J and Duckwiler G R 2000 X-ray videodensitometric methods for blood flow and velocity measurement: a critical review of literature *Med. Phys.* **27** 2008–23
- Shroy R E, Van Lysel M S and Yaffe M J 2000 61 X-ray *The Biomedical Engineering Handbook* 2nd edn (Boca Raton, FL: CRC Press) section VII ([http://engnetbase.com/ejournals/books/book_summary/summary.asp?id = 402](http://engnetbase.com/ejournals/books/book_summary/summary.asp?id=402))
- Smedby O 1992 Angiographic methods for the study of fluid mechanical factors in atherogenesis *Acta Radiol. Suppl.* **380** 1–38
- Tarver D S and Plant G R 1995 Case report: the effect of contrast density on computed tomographic arterial portography *Br. J. Radiol.* **68** 200–3
- Tenjin H, Asakura F, Nakahara Y, Matsumoto K, Matsuo T, Urano F and Ueda S 1998 Evaluation of intraaneurysmal blood velocity by time-density curve analysis and digital subtraction angiography *AJNR* **19** 1303–07
- Wakhloo A K, Schellhammer F, de Vries J, Haberstroh J and Schumacher M 1994 Self-expanding and balloon-expandable stents in the treatment of carotid aneurysms: an experimental study in a canine model *AJNR. Am. J. Neuroradiol.* **15** 493–502
- Wakhloo A K, Lanzino G, Lieber B B and Hopkins L N 1998 Stents for intracranial aneurysms: the beginning of a new endovascular era? *Neurosurgery* **43** 377–9
- Wang Z, Ionita C, Rudin S, Hoffmann K R, Paxton A B and Bednarek D R 2004 Angiographic analysis of blood flow modification in cerebral aneurysm models with a new asymmetric stent *Proc. SPIE* **5369** 307–18